Supplementary Material

Enhancing the Uniformity of $CuBi_2O_4$ Thin Film for Photoelectrochemical (PEC) Water Splitting through Urea-Modified Ethylene Glycol Electrolyte

Xiuru Yang[a], Mansour Alhabradi[bc], Anurag Roy[b], Manal Alruwaili[bd], David Benson[b], Hong Chang[a], Xiaohong Li[b], Asif Ali Tahir*[b], Yanqiu Zhu*[a]

*Corresponding authors

[a] Faculty of Environment, Science and Economy, University of Exeter, Exeter EX4 4QF, UK

[b] Faculty of Environment, Science and Economy, University of Exeter, Penryn TR10 9FE, UK

[c] Department of Physics, Faculty of Science, Majmaah University, Majmaah, 11952, Saudi Arabia

[d] Department of Physics, Faculty of Science, Jouf University, 2014, Sakaka 42421, Saudi Arabia

E-mail: Y.Zhu@exeter.ac.uk

As depicted in the **Table S1**, in order to fabricate the $CuBi_2O_4$ thin film with enhanced PEC water splitting ability, the total concentration of the Bi $(NO_3)_3 \cdot 5H_2O$ and $CuCl_2$ and the deposition time (thickness) controlled by charge deposition repeat cycles have been investigated, before using urea to modify the $CuBi_2O_4$ thin film. The XRD patterns of the thin films produced in different concentrations of the Bi $(NO_3)_3 \cdot 5H_2O$ and $CuCl_2$ or produced with different thickness controlled by different charge deposition cycles, shown in **Fig. S1**, are all in good agreement with the characteristic tetragonal $CuBi_2O_4$ phase (PDF#48-1886), with space group of P4/ncc.[1,2] There were no impurity peaks or phase shifts visible, implying that all thin films synthesized under the conditions shown in **Table S1** were pure $CuBi_2O_4$ phase.

The J-V plots shown in **Fig. S2** were used to investigate the effect of electrolyte concentration and thickness on the PEC performance of the prepared $CuBi_2O_4$ thin films. As displayed in **Fig. S2a**, the prepared 6C-6mM $CuBi_2O_4$ thin film has a highest photocurrent density of -0.96 mA/cm^2, followed by -0.94 mA/cm^2 of 6C-9mM and -0.79 mA/cm^2 of 6C-12mM $CuBi_2O_4$ thin film, under the potential of -0.439 V vs. Ag/AgCl or 0.525 V vs. RHE. Taking the electroplating efficiency and the small photocurrent density difference into account, the 6C-9mM $CuBi_2O_4$ thin film was used to investigate the influence of the charge deposition cycles. As shown in **Fig. S2b**, the photocurrent density of the $CuBi_2O_4$ thin film prepared with 6 cycles charge deposition is -0.94 mA/cm^2, which is greater than the -0.78 and -0.50 mA/cm^2 of the $CuBi_2O_4$ thin film prepared with 5 and 7 cycles charge deposition, respectively. As a result, the 6C-9mM $CuBi_2O_4$ thin film was used to investigate the changes in PEC properties caused by using urea.

Table S1 $CuBi_2O_4$ thin films synthesized in different conditions.

Sample name	Electrolyte	Charge deposition cycles	Calcination condition
6C-6mM	6 mM (Cu: Bi = 1: 2) EG	6	550 °C 2 h
6C-9mM	9 mM (Cu: Bi = 1: 2) EG	6	550 °C 2 h
6C-12mM	12 mM (Cu: Bi = 1: 2) EG	6	550 °C 2 h
5C-9mM	9 mM (Cu: Bi = 1: 2) EG	5	550 °C 2 h
7C-9mM	9 mM (Cu: Bi = 1: 2) EG	7	550 °C 2 h

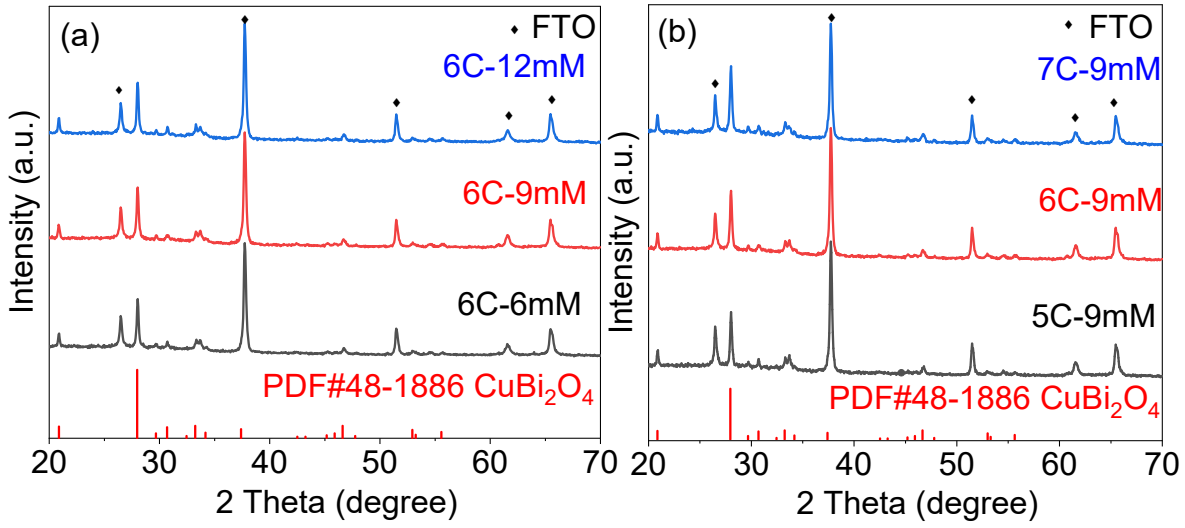

Fig. S1 XRD patterns of prepared $CuBi_2O_4$ thin films on FTO substrate.

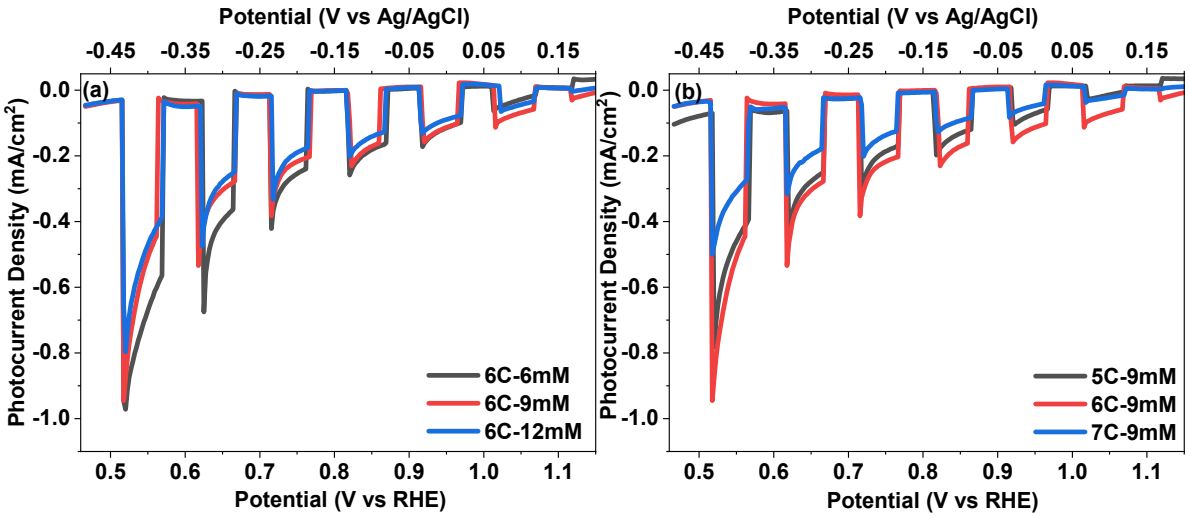

Fig. S2 Photocurrent density-potential vs. RHE or Ag/AgCl (*J-V*) plots under chopped illumination condition.

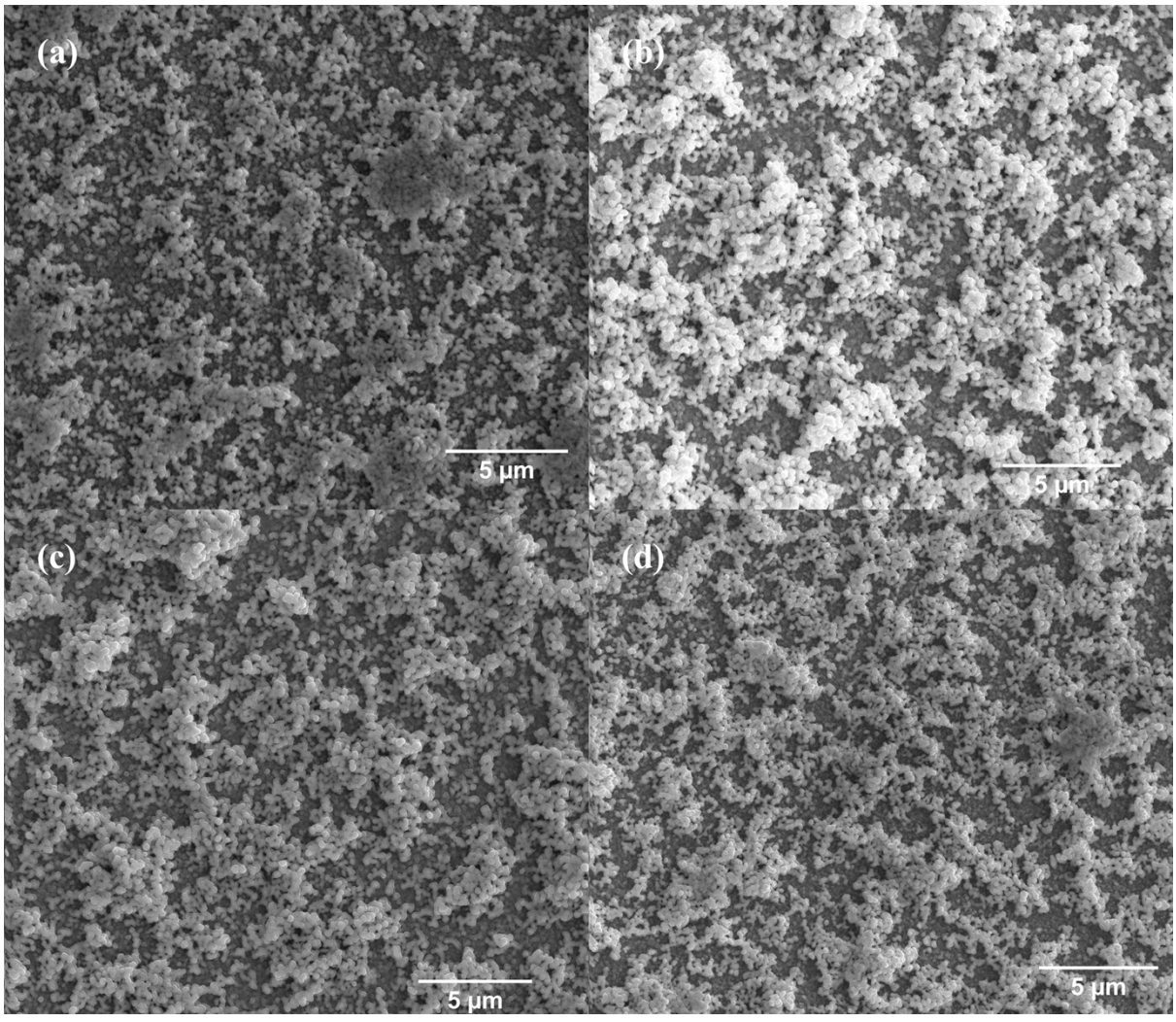

Fig. S3 The low-resolution SEM images of the produced samples: (a) 0 g-urea-6C-9mM; (b) 0.1 g-urea-6C-9mM, (c) 0.15 g-urea-6C-9mM, and (d) 0.2 g-urea-6C-9mM.

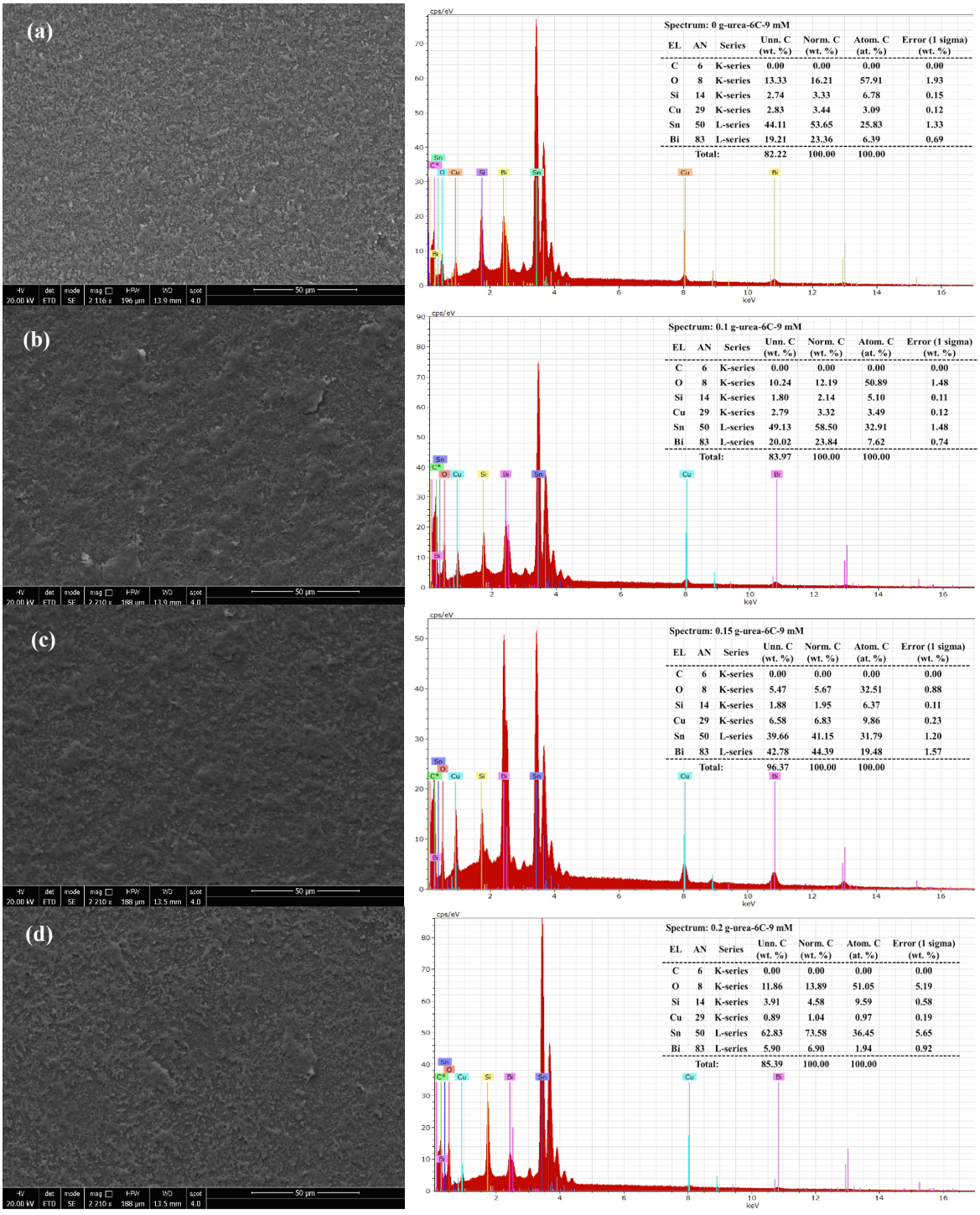

Fig. S4 SEM images and EDS spectra of prepared thin films: (a) 0 g-urea-6C-9mM; (b) 0.1 g-urea-6C-9mM, (c) 0 g-urea-6C-9mM, and (d) 0.2 g-urea-6C-9mM.

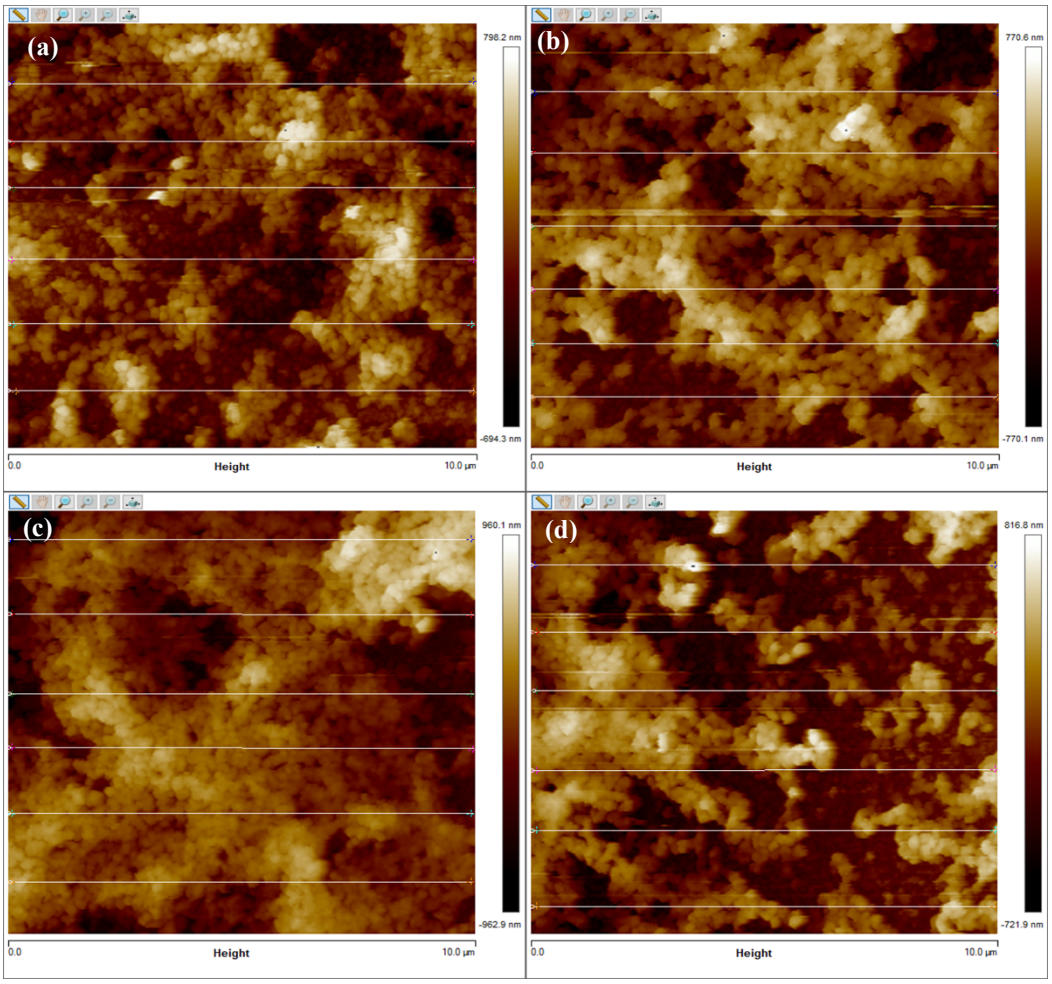

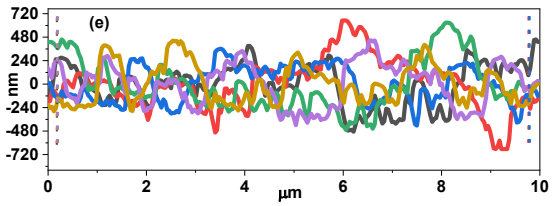

Pair	Horizontal Distance/µm	Vertical Distance/n	Rmax/nm	Ra (Freguency Cutoff)/nm
1	9.804	357.891	938.074	170.432
2	9.804	-114.022	1317.061	198.116
3	9.765	69.066	786.547	162.759
4	9.804	-461.32	1097.276	202.134
5	9.804	-199.906	867.832	185.377
6	9.765	211.733	718.798	167.851
Average Ra/nm				181.1

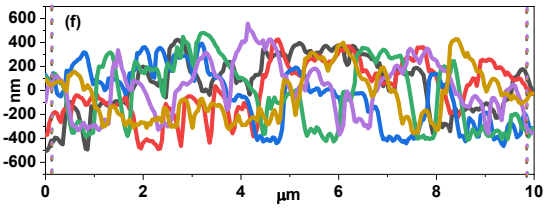

Pair	Horizontal Distance/µm	Vertical Distance/nm	Rmax/nm	Ra (Freguency Cutoff)/nm
1	9.922	473.732	897.57	190.368
2	9.922	239.204	816.055	146.492
3	9.961	-419.581	764.155	144.042
4	9.922	-401.637	938.052	219.845
5	9.922	-411.114	933.195	181.338
6	9.882	-82.558	788.453	167.584
Average Ra/nm				174.9

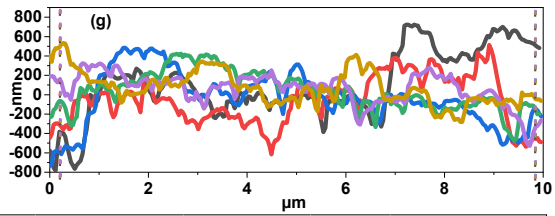

Pair	Horizontal Distance/µm	Vertical Distance/nm	Rmax/nm	Ra (Freguency Cutoff)/nm
1	9.882	1158	1015	209
2	9.922	-78	1069	193
3	10	515	1279	184
4	9.922	56	824	128
5	9.922	-509	743	102
6	9.882	-388	661	109
Average Ra/nm				154.2

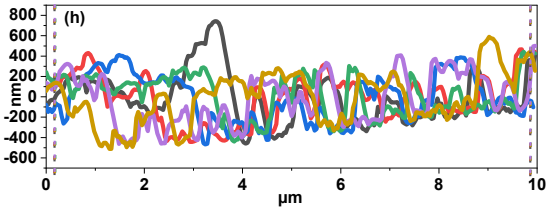

Pair	Horizontal Distance/µm	Vertical Distance/nm	Rmax/nm	Ra (Freguency Cutoff)/nm
1	9.882	358.01	1186.899	174.824
2	9.843	329.752	892.814	193.786
3	9.843	77.753	898.088	192.245
4	9.843	286.691	988.206	154.166
5	9.843	424.858	832.594	202.069
6	9.843	306.188	803.695	193.739
Average Ra/nm				185.1

Fig. S5 AFM 2D perspectives and roughness along the section lines of (a), (e) 0 g-urea-6C-9mM; (b), (f) 0.1 g-urea-6C-9mM; (c), (g) 0.15 g-urea-6C-9mM; and (d), (h) 0.2 g-urea-6C-9mM.

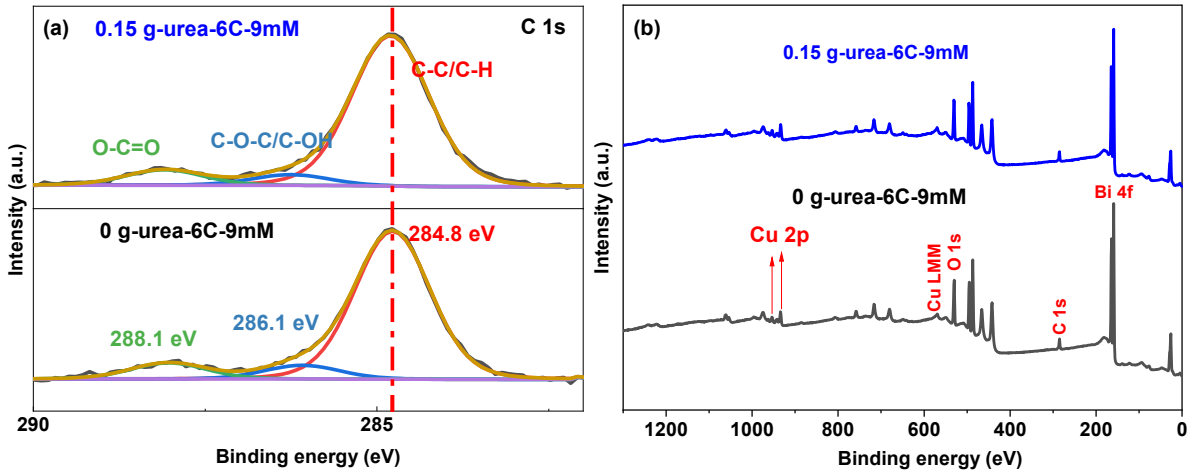

Fig. S6 XPS spectra of prepared $CuBi_2O_4$ thin films: 0 g-urea-6C-9mM and 0.15 g-urea-6C-9mM. (a) C 1s and (b) survey scan.

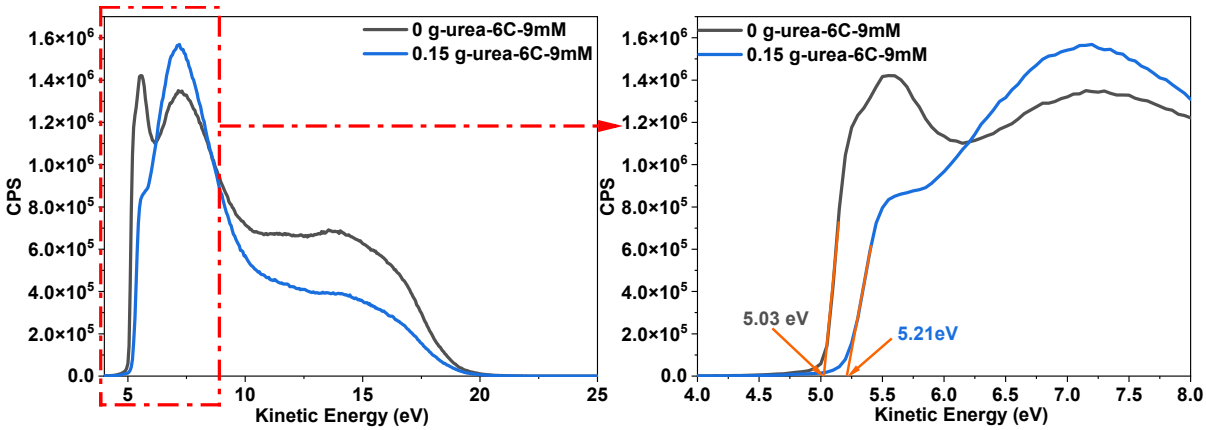

Fig. S7 Ultraviolet photoelectron spectra (UPS) for $CuBi_2O_4$ thin films: 0 g-urea-6C-9mM and 0.15 g-urea-6C-9mM.

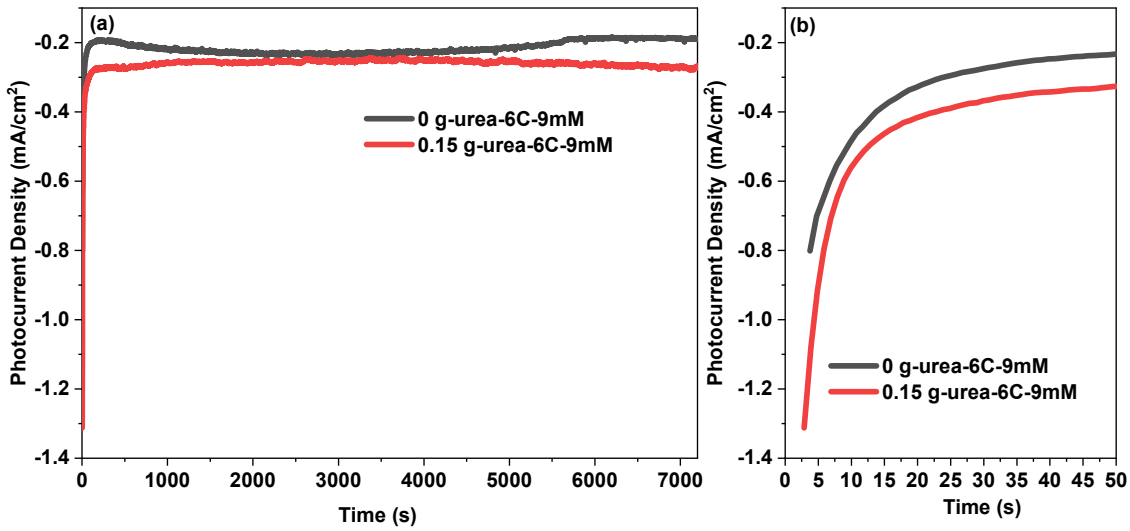

Fig. S8 I-t stability curves determined by Chronoamperometry measurement for the prepared $CuBi_2O_4$ thin films.

Table S2 Photocurrent density of 0.15 g-urea-6C-9mM $CuBi_2O_4$ thin film compared with the photocurrent densities of previously synthesised $CuBi_2O_4$ thin films.

Photocathode	**Photocurrent density (mA/cm^2)**	**Potential (V vs. RHE)**	**Electrolyte**	**Ref.**
FTO/Au/$CuBi_2O_4$/Pt	-0.85	0.25 V	0.1 M Na_2SO_4	[3]
$CuBi_2O_4$ inverse opals	-0.8	0.5 V	0.1 M $KHCO_3$ with 0.1 M $Na_2S_2O_8$	[4]
$CuBi_2O_4$	-0.68	0.25 V	0.132 M KOH and 0.05 M KCl (Ar gas)	[5]
Dendritic $CuBi_2O_4$ Array	-0.83	0.2 V	0.1 M Na_2SO_4 (N_2 gas)	[6]
$CuBi_2O_4$/polythiophene	-0.41	0.3 V	0.3 M K_2SO_4 and 0.2 M phosphate buffer	[7]
High Surface Area $CuBi_2O_4$	-1.0	0.6 V	0.1 M NaOH saturated with O_2	[8]
$CuBi_2O_4$	-0.5	0.4 V	0.3 M K_2SO_4 and 0.2 M phosphate buffer (Ar gas)	[9]
$CuBi_2O_4$	-1.44	0.52 V	0.1 M NaOH	This work

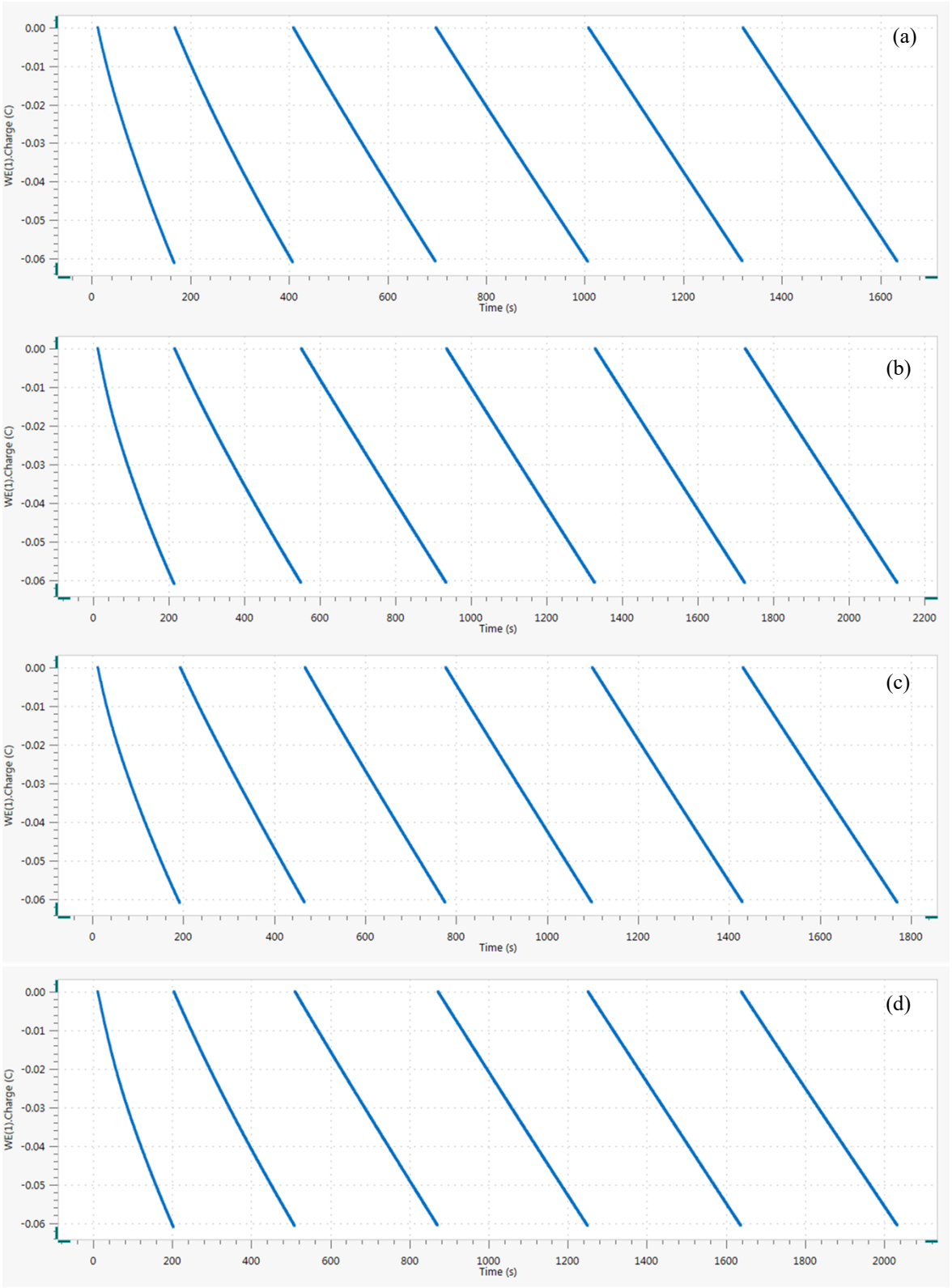

Fig. S9 Electrodeposition procedures: Charge (C) vs. Time (s) curves of prepared thin films (a) 0 g-urea-6C-9mM (b) 0.1 g-urea-6C-9mM (c) 0.15 g-urea-6C-9mM and (d) 0.2 g-urea-6C-9mM.

Reference

1. L. Zhao, X. Wang and Z. Liu, *Appl. Phys. A*, 2018, 124, 836, https://doi.org/10.1007/s00339-018-2262-5.

2. J. Lee, H. Yoon, K. S. Choi, S. Kim, S. Seo, J. Song, B. U. Choi, J. Ryu, S. Ryu, J. Oh, C. Jeon and S. Lee, *Small*, 2020, 16, e2002429, https://doi.org/10.1002/smll.202002429.

3. D. Cao, N. Nasori, Z. Wang, Y. Mi, L. Wen, Y. Yang, S. Qu, Z. Wang and Y. Lei, *J. Mater. Chem. A*, 2016, 4, 8995-9001, https://doi.org/10.1039/c6ta01234e.

4. M. Sun, W. Chen, X. Jiang, B. Liu, B. Tan, L. Luo, M. Xie and Z. Zhang, *ACS Appl. Mater. Interfaces*, 2022, 14, 43946-43954, https://doi.org/10.1021/acsami.2c12309.

5. M. Li, X. Tian, X. Zou, X. Han, C. Du and B. Shan, *Int. J. Hydrog. Energy*, 2020, 45, 15121-15128, https://doi.org/10.1016/j.ijhydene.2020.03.242.

6. Q. Zhang, B. Zhai, Z. Lin, X. Zhao and P. Diao, *J. Phys. Chem. C*, 2021, 125, 1890-1901, https://doi.org/10.1021/acs.jpcc.0c10421.

7. N. Xu, F. Li, L. Gao, H. Hu, Y. Hu, X. Long, J. Ma and J. Jin, *Int. J. Hydrog. Energy*, 2018, 43, 2064-2072, https://doi.org/10.1016/j.ijhydene.2017.12.036.

8. D. Kang, J. C. Hill, Y. Park and K.-S. Choi, *Chem. Mater.*, 2016, 28, 4331-4340, https://doi.org/10.1021/acs.chemmater.6b01294.

9. S. P. Berglund, F. F. Abdi, P. Bogdanoff, A. Chemseddine, D. Friedrich and R. van de Krol, *Chem. Mater.*, 2016, 28, 4231-4242, https://doi.org/10.1021/acs.chemmater.6b00830.